

Unpacking Information Bottlenecks: Unifying Information-Theoretic Objectives in Deep Learning

Andreas Kirsch Clare Lyle Yarín Gal
OATML

Department of Computer Science
University of Oxford

{andreas.kirsch, clare.lyle, yarin}@cs.ox.ac.uk

Abstract

The information bottleneck (IB) principle offers both a mechanism to explain how deep neural networks train and generalize, as well as a regularized objective with which to train models. However, multiple competing objectives have been proposed based on this principle, and the information-theoretic quantities in these objectives are difficult to compute for large deep neural networks. This, in turn, limits their use as a training objective. In this work, we review these quantities, compare and unify previously proposed objectives and relate them to surrogate objectives more friendly to optimization. We find that these surrogate objectives allow us to apply the information bottleneck to modern neural network architectures. We demonstrate our insights on Permutation-MNIST, MNIST and CIFAR10.

1 Introduction

The Information Bottleneck (IB) principle, introduced by Tishby et al. (2000), proposes that training and generalization in deep neural networks (DNNs) can be explained by information-theoretic principles (Tishby & Zaslavsky, 2015; Shwartz-Ziv & Tishby, 2017; Achille & Soatto, 2018a). The IB principle suggests that learning consists of two competing objectives: maximizing the mutual information between the latent representation and the label to promote accuracy while at the same time minimizing the mutual information between the latent representation and the input to promote generalization. Recent work has tied this intuition to both unsupervised and self-supervised learning (Oord et al., 2018; Belghazi et al., 2018; Zhang et al., 2018, among others).

Following this principle, many variations of IB objec-

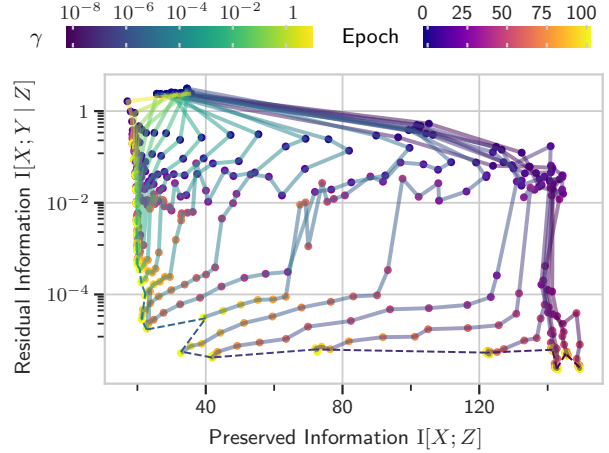


Figure 1: *Information Plane Plot of training trajectories for ResNet18 models on CIFAR10.* We use the surrogate objective $\min_{\Theta} H_{\Theta}[Y | Z] + \gamma \mathbb{E} \|Z\|^2$ from section 6. Trajectories (for every 5th epoch) are plotted for different γ . The lines are colored by γ , the dots by epoch. The dashed line is the saturation curve depicted in figure 6. Depending on γ , different levels of compression (Preserved Information ↓) are achieved, which trade-off with performance (Residual Information ↓). See section 7.3.

tives have been proposed (Alemi et al., 2016; Strouse & Schwab, 2017; Fisher, 2019; Gondek & Hofmann, 2003; Achille & Soatto, 2018a), which, in supervised learning, have been demonstrated to benefit robustness to adversarial attacks (Alemi et al., 2016; Fisher, 2019), generalization and regularization against overfitting to random labels (Fisher, 2019). However, whether the benefits of training with the IB objective are due to the IB principle, or some other unrelated mechanism, remains unclear (Saxe et al., 2019; Amjad & Geiger, 2019; Tschannen et al., 2019). Critical to learning with IB objectives is the computation of the information-theoretic quantities¹ used. While progress has been made in developing mutual information

¹We shorten these to *information quantities* from now on.

estimators for DNNs (Poole et al., 2019; Belghazi et al., 2018; Noshad et al., 2019; McAllester & Stratos, 2018; Kraskov et al., 2004), current methods still face many limitations when concerned with high-dimensional random variables (McAllester & Stratos, 2018). This presents an additional challenge to training with IB objectives.

In this paper, we analyze information quantities and relate them to surrogate objectives for the IB principle which are more friendly to optimization. In the process, we review commonly-used information quantities for which we provide mathematically grounded intuition via information diagrams in section 2 and 3, and unify several variations of the IB objective in section 4. Chief among these information quantities are $H[Y|Z]$ and $H[Z|Y]$, which we label **Decoder Uncertainty** and **Reverse Decoder Uncertainty**, respectively, and which act as main loss and regularization terms. We demonstrate in section 5 that using the **Decoder Uncertainty** as a training objective can minimize the training error and show how to upper-bound and estimate it efficiently for well-known DNN architectures by expanding on the findings of Alemi et al. (2016) to connect it to the commonly-used cross-entropy loss² and Dropout regularization. In section 6, we examine pathologies of differential entropies and investigate how the **Reverse Decoder Uncertainty** can be optimized using surrogate terms, which leads to a simple and tractable surrogate IB objective. In section 7, we provide experiments to validate our insights qualitatively and quantitatively on Permutation-MNIST, MNIST and CIFAR10, and obtain information plane plots similar to those predicted by Tishby & Zaslavsky (2015)—for example in figure 1.

Compared to existing research, we show that we can optimize IB objectives for well-known DNN architectures using standard optimizers, losses and regularizers, without needing complex estimators or generative models.

2 Information Quantities & Information Diagrams

To unify previous work and demonstrate how different IB objectives relate to each other, we first need to introduce some notation and terminology. Here we review well-known information quantities and provide intuition using information diagrams (Yeung, 1991).

We denote entropy $H[\cdot]$, joint entropy $H[\cdot, \cdot]$, conditional entropy $H[\cdot|\cdot]$, mutual information $I[\cdot; \cdot]$ and Shannon’s information content $h(\cdot)$ (Cover & Thomas, 2012; MacKay, 2003; Shannon, 1948) :

$$h(x) = -\ln x$$

²This connection was assumed without proof by Achille & Soatto (2018a,b).

$$\begin{aligned} H[X] &= \mathbb{E}_{p(x)} h(p(x)) \\ H[X, Y] &= \mathbb{E}_{p(x,y)} h(p(x, y)) \\ H[X|Y] &= H[X, Y] - H[Y] \\ &= \mathbb{E}_{p(y)} H[X|y] = \mathbb{E}_{p(x,y)} h(p(x|y)) \\ I[X; Y] &= H[X] + H[Y] - H[X, Y] \\ &= \mathbb{E}_{p(x,y)} h\left(\frac{p(x)p(y)}{p(x,y)}\right) \\ I[X; Y|Z] &= H[X|Z] + H[Y|Z] - H[X, Y|Z], \end{aligned}$$

where X, Y, Z are random variables and x, y, z are outcomes these random variables can take. We are going to use differential entropies interchangeably with entropies. Equalities hold as can be verified via symbolic expansions and inequalities in the differential setting will be covered in section 6.1.

We will further require the Kullback-Leibler divergence $D_{KL}(\cdot \| \cdot)$ and cross-entropy $H(\cdot \| \cdot)$:

$$\begin{aligned} H(p(x) \| q(x)) &= \mathbb{E}_{p(x)} h(q(x)) \\ D_{KL}(p(x) \| q(x)) &= \mathbb{E}_{p(x)} h\left(\frac{q(x)}{p(x)}\right) \\ H(p(y|x) \| q(y|x)) &= \mathbb{E}_{p(x)} \mathbb{E}_{p(y|x)} h(q(y|x)) \\ &= \mathbb{E}_{p(x,y)} h(q(y|x)) \\ D_{KL}(p(y|x) \| q(y|x)) &= \mathbb{E}_{p(x,y)} h\left(\frac{q(y|x)}{p(y|x)}\right) \end{aligned}$$

2.1 Information Diagrams

Information diagrams (I-diagrams), like the one depicted in figure 2, visualize the relationship between information quantities: Yeung (1991) shows that we can define a signed measure μ^* such that these well-known quantities map to abstract sets and are consistent with set operations.

$$\begin{aligned} H[A] &= \mu^*(A) \\ H[A_1, \dots, A_n] &= \mu^*(\cup_i A_i) \\ H[A_1, \dots, A_n | B_1, \dots, B_n] &= \mu^*(\cup_i A_i - \cup_i B_i) \\ I[A_1; \dots; A_n] &= \mu^*(\cap_i A_i) \\ I[A_1; \dots; A_n | B_1, \dots, B_n] &= \mu^*(\cap_i A_i - \cup_i B_i) \end{aligned}$$

Note that interaction information (McGill, 1954) follows as canonical generalization of the mutual information to multiple variables from that work, whereas total correlation does not.

While equalities can be read off directly from I-diagrams, inequalities need to be treated with care because the mutual information of more than two random variables can be negative. On the other hand, all quantities in one or two variables are non-negative by definition, or can be made so in the continuous case, as we will discuss in detail in section 6.1.

When applying set intuitions, some caution is warranted as well. As the signed measure can be negative, $\mu^*(X \cap$

Thus, all the quantities in the diagram are positive, which allows us to read off inequalities as well⁴. In section 4, we will make use of the following composite information quantities to simplify IB objectives:

Relevant Information $I[X; Y] = I[X; Y | Z] + I[Y; Z]$ quantifies the information in the data that is relevant for the labels and which our model needs to capture to be able to predict the labels.

Preserved Information $I[X; Z] = I[X; Z | Y] + I[Y; Z]$ quantifies information from the data that is preserved in the latent.

Decoder Uncertainty $H[Y | Z] = I[X; Y | Z] + H[Y | X]$ quantifies the uncertainty about the labels after learning about the latent Z . If $H[Y | Z]$ reaches 0, it means that no additional information is needed to infer the correct label Y from the latent Z : the optimal decoder can be a deterministic mapping. Intuitively, we want to minimize this quantity for good predictive performance.

Reverse Decoder Uncertainty $H[Z | Y] = I[X; Z | Y] + H[Z | X]$ quantifies the uncertainty about the latent Z given the label Y . We can imagine training a new model to predict Z given Y and minimizing $H[Z | Y]$ to 0 would allow for a deterministic decoder from the latent to given the label.

Nuisance⁵ $H[X | Y] = H[X | Y, Z] + I[X; Z]$ quantifies the information in the data that is not relevant for the task (Achille & Soatto, 2018a).

We will further refer to six atomic quantities:

Label Uncertainty $H[Y | X]$ quantifies the uncertainty in our labels. If we have multiple labels for the same data sample, it will be > 0 . It is 0 otherwise.

Encoding Uncertainty $H[Z | X]$ quantifies the uncertainty in our latent encoding given a sample. When using a Bayesian model with random variable ω for the weights, one can further split this term into $H[Z | X] = I[Z; \omega | X] + H[Z | X, \omega]$, so uncertainty stemming from weight uncertainty and independent noise (Houlsby et al., 2011; Kirsch et al., 2019).

Preserved Relevant Information $I[Y; Z]$ quantifies information in the latent that is relevant for our task of predicting the labels (Tishby & Zaslavsky, 2015). Intuitively, we want to maximize it for good predictive performance.

Residual Information $I[X; Y | Z]$ quantifies information for the labels that is not captured by the latent (Tishby & Zaslavsky, 2015) but would be useful to be captured.

Redundant Information $I[X; Z | Y]$ quantifies information in the latent that is not needed for predicting the labels⁶.

In the next section, we will make use of these to discuss IB objectives.

4 Information Bottleneck & Related Works

4.1 Goals & Motivation

The IB principle from Tishby et al. (2000) can be recast as a generalization of finding minimal sufficient statistics for the labels given the data (Shamir et al., 2010; Tishby & Zaslavsky, 2015; Fisher, 2019): it strives for minimality and sufficiency of the latent Z . Minimality is about minimizing amount of information necessary of X for the task, so minimizing the **Preserved Information** $I[X; Z]$; while sufficiency is about preserving the information to solve the task, so maximizing the **Preserved Relevant Information** $I[Y; Z]$.

From figure 2, we can read off the definitions of **Relevant Information** and **Preserved Information**:

$$I[X; Y] = I[Y; Z] + I[X; Y | Z] \quad (2)$$

$$I[X; Z] = I[Y; Z] + I[X; Z | Y], \quad (3)$$

and see that maximizing the **Preserved Relevant Information** $I[Y; Z]$ is equivalent to minimizing the **Residual Information** $I[X; Y | Z]$, while minimizing the **Preserved Information** $I[X; Z]$ at the same time means minimizing the **Redundant Information** $I[X; Z | Y]$, too, as $I[X; Y]$ is constant for the given dataset⁷. Moreover, we also see that the **Preserved Relevant Information** $I[Y; Z]$ is upper-bounded by **Relevant Information** $I[X; Y]$, so to capture all relevant information in our latent, we want $I[X; Y] = I[Y; Z]$.

Using the diagram, we can also see that minimizing the **Residual Information** is the same as minimizing the **Decoder Uncertainty** $H[Y | Z]$:

$$I[X; Y | Z] = H[Y | Z] - H[Y | X].$$

Ideally, we also want to minimize the **Encoding Uncertainty** $H[Z | X]$ to find the most deterministic latent encoding Z . Minimizing the **Encoding Uncertainty** and the

⁴See section 6.1 for how to deal with continuous Z .

⁵Not depicted in figure 2.

⁶Fisher (2019) uses the term ‘‘Residual Information’’ for this, which conflicts with Tishby & Zaslavsky (2015).

⁷That is, it does not depend on Θ .

Redundant Information $I[X; Z | Y]$ together is the same as minimizing the Reverse Decoder Uncertainty $H[Z | Y]$.

All in all, we want to minimize both the Decoder Uncertainty $H[Y | Z]$ and the Reverse Decoder Uncertainty $H[Z | Y]$. We will see that IB objectives are doing that in section 4.3.

4.2 IB Objectives

“The Information Bottleneck Method” (IB)

Tishby et al. (2000) introduce $MI(X; \hat{X}) - \beta MI(\hat{X}; Y)$ as optimization objective for the Information Bottleneck. We can relate this to our notation by renaming $\hat{X} = Z$, such that the objective becomes

$$\min I[X; Z] - \beta I[Y; Z].$$

The IB objective minimizes the Preserved Information $I[X; Z]$ and trades it off with maximizing the Preserved Relevant Information $I[Y; Z]$. Tishby & Zaslavsky (2015) mention that the IB objective is equivalent to minimizing $I[X; Z] + \beta I[X; Y | Z]$, see our discussion above. Tishby et al. (2000) provide an optimal algorithm for the tabular case, when X , Y and Z are all categorical. This has spawned additional research to optimize the objective for other cases and specifically for DNNs.

“Deterministic Information Bottleneck” (DIB)

Strouse & Schwab (2017) introduce as objective

$$\min H[Z] - \beta I[Y; Z].$$

Compared to the IB objective, this also minimizes $H[Z | X]$ and encourages determinism. Vice-versa, for deterministic encoders, $H[Z | X] = 0$, and their objective matches the IB objective. Like Tishby et al. (2000), they provide an algorithm for the tabular case. As we will see in section 6.1, it does not easily translate to a continuous latent Z .

“Deep Variational Information Bottleneck”

Alemi et al. (2016) rewrite the terms in the bottleneck as maximization problem “ $\max I[Y; Z] - \beta I[X; Z]$ ” and swap the β parameter. Their β would be $1/\beta$ in IB above, which emphasizes that $I[Y; Z]$ is important for performance and $I[X; Z]$ acts as regularizer. They explicitly model $p(z | x)$ and regularize it to become a unit Gaussian, and they variationally approximate $p_\theta(\hat{y} | z)$. We will recover both parts of their objective in section 5.2 and section 6.2.

“Conditional Entropy Bottleneck”

Fisher (2019) introduce their Conditional Entropy Bottleneck as “ $\min I[X; Z | Y] - I[Y; Z]$ ”. We can rewrite

the objective as $I[X; Z | Y] + I[X; Y | Z] - I[X; Y]$, using equation 2 and equation 3. The last term is constant for the dataset and can thus be dropped. Likewise, the IB objective can be rewritten as minimizing $I[X; Z | Y] + (\beta - 1)I[X; Y | Z]$. The two match for $\beta = 2$. Fisher (2019) provides experimental results that favorably compare to Alemi et al. (2016), possibly due to additional flexibility as Fisher (2019) do not constrain $p(z)$ to be a unit Gaussian and employ variational approximations for all terms.

4.3 Another Look at IB & DIB

We now expand the IB and DIB objectives into “disjoint” terms and drop constant ones to find a more canonical form. This will lead us to focus on the optimization of the Decoder Uncertainty $H[Y | Z]$ along with additional regularization terms. In section 5, we will discuss the properties of $H[Y | Z]$, and in section 6 we will examine the regularization terms.

Observation 1. For IB, we obtain

$$\begin{aligned} \arg \min I[X; Z] - \beta I[Y; Z] \\ &= \arg \min I[X; Z | Y] + (\beta - 1)H[Y | Z] \\ &= \arg \min H[Y | Z] + \beta' I[X; Z | Y] \\ &= \arg \min H[Y | Z] + \beta'(H[Z | Y] - H[Z | X]), \quad (\text{IB}) \end{aligned}$$

and, for DIB,

$$\begin{aligned} \arg \min H[Z] - \beta I[Y; Z] \\ &= \arg \min H[Z | Y] + (\beta - 1)H[Y | Z] \\ &= \arg \min H[Y | Z] + \beta' H[Z | Y], \quad (\text{DIB}) \end{aligned}$$

with $\beta' := \frac{1}{\beta - 1} \in [0, \infty)$.

We implicitly limit ourselves to $\beta \geq 1$ (and allow for $\beta \rightarrow \{1, \infty\}$). For $\beta < 1$, we would be maximizing the Decoder Uncertainty, which does not make sense: the trivial solution to this is one where Z contains no information on Y ⁸.

We can also show for DIB

$$\begin{aligned} \arg \min H[Z] - \beta I[Y; Z] \\ &= \arg \min H[Z] + \beta H[Y | Z] \\ &= \arg \min H[Y | Z] + \beta'' H[Z], \end{aligned}$$

with $\beta'' := \frac{1}{\beta} \in [0, \infty)$, which will be relevant in section 6.

The Decoder Uncertainty $H[Y | Z]$ provides a loss term, and the Reverse Decoder Uncertainty $H[Z | Y]$ and Redundant Information $I[X; Z | Y] = H[Z | Y] - H[Z | X]$, respectively, provide a regularization term. We will compare this

⁸In the case of DIB, the trivial solution is to map every input deterministically to a single value; whereas for IB, we only minimize the Redundant Information, and an optimal solution has no information on Y while being free to contain noise.

to the common objective of minimizing the cross-entropy together with L_2 regularization of Z : section 5 will examine $H[Y | Z]$ as main loss term and how to optimize it efficiently, while section 6 will discuss regularization.

5 Decoder Uncertainty $H[Y | Z]$

This section will show that the **Decoder Uncertainty** $H[Y | Z]$ is a useful loss term that can bound the (training) error and which we can upper-bound and minimize using the **Decoder Cross-Entropy** which is introduced below. This shows a path to minimizing $H[Y | Z]$ when its direct computation is not feasible. We will relate this objective to the commonly used Dropout regularization technique (Srivastava et al., 2014) in section 5.3.

We will refer to the common cross-entropy introduced in section 3.1 as **Prediction Cross-Entropy**, denoted $H_\Theta[Y | X]$, and introduce the **Decoder Cross-Entropy**, denoted $H_\Theta[Y | Z]$, which focuses on $p_\Theta(\hat{y} | z)$ ⁹. Note the difference to the conditional entropy and that we use Θ as subscript to denote dependence on the model.

Prediction Cross-Entropy $H_\Theta[Y | X]$

$$\begin{aligned} H_\Theta[Y | X] &:= H(\hat{p}(y | x) \| p_\Theta(\hat{Y} = y | x)) \\ &= \mathbb{E}_{\hat{p}(x,y)} h(p_\Theta(\hat{Y} = y | x)) \\ &= \mathbb{E}_{\hat{p}(x,y)} h(\mathbb{E}_{p_\Theta(z|x)} p_\Theta(\hat{Y} = y | z)) \end{aligned}$$

Decoder Cross-Entropy $H_\Theta[Y | Z]$

$$\begin{aligned} H_\Theta[Y | Z] &:= H(p(y | z) \| p_\Theta(\hat{Y} = y | z)) \\ &= \mathbb{E}_{p(y,z)} h(p_\Theta(\hat{Y} = y | z)) \\ &= \mathbb{E}_{\hat{p}(x,y)} \mathbb{E}_{p_\Theta(z|x)} h(p_\Theta(\hat{Y} = y | z)) \end{aligned}$$

Observation 2. Using Jensen’s inequality on convex $h(x) = -\ln x$, we see that the **Prediction Cross-Entropy** is always less or equal to the **Decoder Cross-Entropy**:

$$H_\Theta[Y | X] \leq H_\Theta[Y | Z]. \quad (4)$$

If a *deterministic encoder* is used instead of a stochastic one, for example a standard deterministic neural network, Jensen’s inequality above becomes an equality:

$$H_\Theta[Y | X] = H_\Theta[Y | Z].$$

Then minimizing the **Decoder Cross-Entropy** $H_\Theta[Y | Z]$ becomes equivalent to minimizing the normal deep learning cross-entropy. The decoder $p_\Theta(\hat{y} | z)$ can be either

⁹This is a suggestive notation for we will show in section 5.2 that $H_\Theta[Y | Z] \geq H[Y | Z]$ and, similarly, $H_\Theta[Y | X] \geq H[Y | X]$, and we can use cross-entropies to approximate conditional entropies.

stochastic by outputting a categorical distribution after a SoftMax layer on top of a deterministic network for a categorical latent, or it can be stochastic by using Dropout, for example.

5.1 Training Error Minimization

To motivate that $H[Y | Z]$ (or $H_\Theta[Y | Z]$) can be used as main loss term, we show that it can bound the (training) error probability since *accuracy* is often the true objective when machine learning models are deployed on real-world problems¹⁰.

Observation 3. We can obtain the following bound for the training error:

$$\begin{aligned} p(\text{“}\hat{Y} \text{ is wrong”}) &\leq 1 - e^{-H_\Theta[Y | Z]} \\ &= 1 - e^{-(H[Y | Z] + D_{KL}(p(y|z) \| p_\Theta(\hat{y}|z)))}. \end{aligned}$$

The derivation is as follows.

$$\begin{aligned} p(\text{“}\hat{Y} \text{ is correct”}) &= \mathbb{E}_{\hat{p}(x,y)} p(\text{“}\hat{Y} \text{ is correct”} | x, y) \\ &= \mathbb{E}_{\hat{p}(x,y)} \mathbb{E}_{p_\Theta(z|x)} p_\Theta(\hat{Y} = y | z) = \mathbb{E}_{p(y,z)} p_\Theta(\hat{Y} = y | z). \end{aligned}$$

We can then use Jensen’s inequality on $h(x) = -\ln x$ again¹¹:

$$\begin{aligned} h(\mathbb{E}_{p(y,z)} p_\Theta(\hat{Y} = y | z)) &\leq \mathbb{E}_{p(y,z)} h(p_\Theta(\hat{Y} = y | z)) \\ \Leftrightarrow p(\text{“}\hat{Y} \text{ is correct”}) &\geq e^{-H(p(y|z) \| p_\Theta(\hat{y}|z))} \\ \Leftrightarrow p(\text{“}\hat{Y} \text{ is wrong”}) &\leq 1 - e^{-H_\Theta[Y | Z]}. \end{aligned}$$

Finally, we split the **Decoder Cross-Entropy** into the **Decoder Uncertainty** and a Kullback-Leibler divergence:

$$H_\Theta[Y | Z] = H[Y | Z] + D_{KL}(p(y | z) \| p_\Theta(\hat{Y} = y | z)).$$

The **Decoder Cross-Entropy** depends on $H[Y | Z]$ and on the divergence between the (learnt) decoder $p_\Theta(\hat{y} | z)$ and the optimal decoder $p(y | z)$. If we can upper-bound this divergence, minimizing the **Decoder Uncertainty** $H[Y | Z]$ becomes a sensible minimization objective as it reduces the probability of misclassification. In section 5.4, we will look at categorical Z for which optimal decoders can be constructed (and the divergence becomes zero).

How can we minimize $H[Y | Z]$ in other cases though, and how large is the gap between $H[Y | Z]$ and $H_\Theta[Y | Z]$? In section 7.1, we report evidence that the gap is small when we pick either of the two as objective. Next we will examine tractable ways to estimate the **Decoder Uncertainty**.

¹⁰As we only take into account the empirical distribution $\hat{p}(x, y)$ available for training, the following derivation refers only to the empirical risk, and not to the expected risk of the estimator \hat{Y} .

¹¹We can similarly show that the training error is bounded by the **Prediction Cross-Entropy** $H_\Theta[Y | X]$.

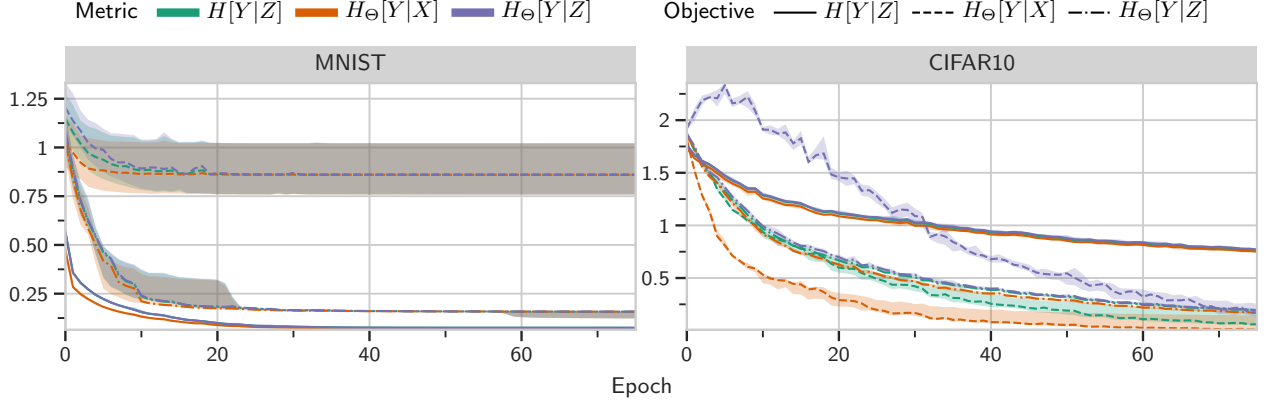


Figure 3: *Decoder Uncertainty*, *Decoder Cross-Entropy* and *Prediction Cross-Entropy* for Permutation-MNIST and CIFAR10 with a categorical Z . $C = 100$ categories are used for Z . We optimize with different minimization objectives in turn and plot the metrics (8 trials, median with confidence bounds for the 25% and 75% quartiles). The gap between $H[Y|Z]$ and $H_{\Theta}[Y|Z]$ becomes small when training with either. When training with $H_{\Theta}[Y|X]$ on CIFAR10, there are significant gaps. See section 7.1 for more details.

5.2 Decoder Uncertainty \leq Decoder Cross-Entropy

By noting the non-negativity of the KL divergence $D_{\text{KL}}(p(y|z) \parallel p_{\Theta}(\hat{Y} = y|z)) \geq 0$ above, we see that the *Decoder Cross-Entropy* upper-bounds the *Decoder Uncertainty*¹², which we can use as proxy to minimize $H[Y|Z]$. This leads us to the following observation.

Observation 4. *The Decoder Cross-Entropy provides an upper bound on the Decoder Uncertainty:*

$$H[Y|Z] \leq H_{\Theta}[Y|Z] = H(p(y|z) \parallel p_{\Theta}(\hat{Y} = y|z)). \quad (5)$$

This is the bound and the term that Alemi et al. (2016) use to variationally approximate $p(y|z)$. We can make this explicit by applying the reparameterization trick:

$$\mathbb{E}_{p_{\Theta}(z|x)} [\cdot(z)] = \mathbb{E}_{p(\epsilon)} [\cdot(z = f_{\Theta}(x, \epsilon))],$$

which yields

$$\begin{aligned} H(p(y|z) \parallel p_{\Theta}(\hat{Y} = y|z)) &= \mathbb{E}_{p(y,z)} h(p_{\Theta}(\hat{Y} = y|z)) \\ &= \mathbb{E}_{\hat{p}(x,y)} \mathbb{E}_{p_{\Theta}(z|x)} h(p_{\Theta}(\hat{Y} = y|z)) \\ &= \mathbb{E}_{\hat{p}(x,y)} \mathbb{E}_{p(\epsilon)} h(p_{\Theta}(\hat{Y} = y|z = f_{\Theta}(x, \epsilon))). \end{aligned}$$

5.3 Dropout Training Minimizes Decoder Uncertainty

DNNs that use Dropout regularization (Srivastava et al., 2014) are stochastic and fit the equation above when we interpret ϵ as the sampled Dropout mask. Within Bayesian

¹² Alternatively, we can use Gibb's inequality $H[p(x)] = H(p(x) \parallel p(x)) \leq H(p(x) \parallel q(x))$, with equality only when $p(x) = q(x)$.

Deep Learning, Monte-Carlo Dropout (Gal & Ghahramani, 2016) specifically estimates the prediction mean $p_{\Theta}(\hat{y}|x)$.

When training with Dropout, usually only a single sample is used, which yields an estimator for both the *Decoder Cross-Entropy* and the *Prediction Cross-Entropy*. Burda et al. (2015) show it is an unbiased estimator for the *Decoder Cross-Entropy* $H_{\Theta}[Y|Z]$, while it only yields a biased estimator for the *Prediction Cross-Entropy* $H_{\Theta}[Y|X]$ (which it upper-bounds).

Observation 5. *When we take only a single Dropout sample during training and minimize a biased estimate for the Prediction Cross-Entropy, which is usually the stated objective, we are actually minimizing an unbiased estimate of $H_{\Theta}[Y|Z]$ and are thus also minimizing the Decoder Uncertainty $H[Y|Z]$.*

This is also the case for multi-sample approaches like Multi-Sample Dropout (Inoue, 2019), which optimizes $H_{\Theta}[Y|Z]$, but not for Importance Weighted Stochastic Gradient Descent (Noh et al., 2017), which optimizes $H_{\Theta}[Y|X]$.

Compared to Alemi et al. (2016) and Achille & Soatto (2018a), which look at special cases, we go further and have shown that $H[Y|Z]$ is minimized in modern DNN architectures that use Dropout by the normal cross-entropy, which is the usual training objective. More generally, we have shown that $H[Y|Z]$ is minimized by the regular *Prediction Cross-Entropy* $H_{\Theta}[Y|X]$ for deterministic models, and by the *Decoder Cross-Entropy* $H_{\Theta}[Y|Z]$ for stochastic models.

What are the differences between optimizing the two

cross-entropies, and is one more amenable than the other to our usual optimization methods based on stochastic gradient descent? We will investigate this question empirically in section 7.1, where we do observe differences between the [Decoder Cross-Entropy](#) and the [Prediction Cross-Entropy](#).

5.4 Categorical Z

To answer the questions from the section 5.1, we need to compute $H[Y | Z]$. For categorical Z , $p(y | z)$ can be computed exactly for a given encoder $p_\theta(z | x)$ by using the empirical data distribution, which, in turn, allows us to compute $H[Y | Z]$ ¹³. This is similar to computing a confusion matrix between Y and Z , and is related to the self-consistent equations in [Tishby et al. \(2000\)](#); [Gondek & Hofmann \(2003\)](#).

Moreover, if we set $p_\theta(\hat{y} | z) := p(Y = \hat{y} | z)$ to have an optimal decoder, we obtain equality in equation 5 and equation 4 becomes

$$H_\theta[Y | X] \leq H_\theta[Y | Z] = H[Y | Z].$$

If the encoder were also deterministic, we would obtain

$$H_\theta[Y | X] = H_\theta[Y | Z] = H[Y | Z].$$

We can minimize $H[Y | Z]$ directly using gradient descent. $\frac{d}{d\theta} H[Y | Z]$ only depends on $p(y | z)$ and $\frac{d}{d\theta} p_\theta(z | x)$:

$$\frac{d}{d\theta} H[Y | Z] = \mathbb{E}_{p(x,z)} \left[\frac{d}{d\theta} [\ln p_\theta(z | x)] \mathbb{E}_{p(y|z)} h(p(y | z)) \right].$$

The derivation can be found in the appendix in section A.3. If we minimize $H[Y | Z]$ directly, we can compute $p(y | z)$ after every training epoch and fix $p_\theta(\hat{y} | z) := p(Y = \hat{y} | z)$ to create the discriminative model $p_\theta(\hat{y} | x)$.

6 Surrogates for the Regularization Terms

IB objectives consist of two terms: an error minimization term $H[Y | Z]$ and a regularization term $H[Z | Y]$ or $I[X; Z | Y]$, respectively. In the previous section, we have examined ways of tractably estimating the error minimization term. In this section, we will first discuss how to minimize entropies meaningfully and show how this unifies DIB and IB via the inequality $I[X; Z | Y] \leq H[Z | Y] \leq H[Z]$ before providing upper-bounds for $H[Z | Y]$ and $H[Z]$, leading to tractable optimization of the regularization term.

6.1 Differential Entropies

Usually, the latent Z is a continuous random variable in many dimensions. In this case, computing information-

¹³ $p(y|z)$ depends on Θ through $p_\theta(z|x)$: $p(y|z) = \frac{\sum_x \hat{p}(x,y) p_\theta(z|x)}{\sum_x \hat{p}(x) p_\theta(z|x)}$.

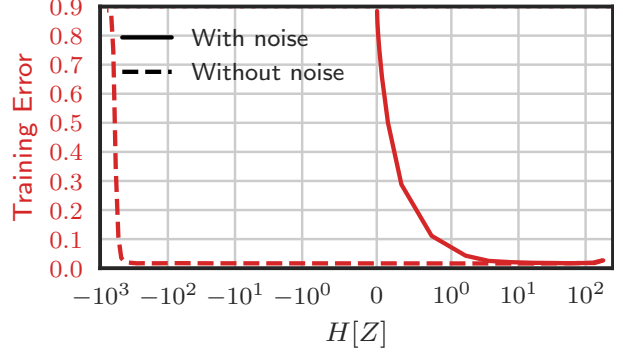


Figure 4: *Scaling the entropy of a noise-free latent does not affect the training error.* Without noise, entropy can decrease freely without change in error rate until it is affected by floating-point issues; when adding zero-entropy noise, the error rate starts increasing gradually and meaningfully as the entropy approaches zero. See section 6.1 and section 7.2 for more details.

theoretic quantities for continuous random variables presents both computational and philosophical challenges. Differential entropies defined on continuous spaces are not bounded from below, unlike entropies on discrete probability spaces. This means that the DIB objective in equation DIB is not guaranteed to have an optimal solution, and allows for pathological optimization trajectories in which the latent variable Z 's variance can be scaled to be arbitrarily small achieving arbitrarily high-magnitude negative entropy. In section 7.2, we provide a toy experiment demonstrating this.

Intuitively, one can interpret this issue as being allowed to encode information in an arbitrarily-small real number using infinite precision, similar to arithmetic coding ([MacKay, 2003](#); [Shwartz-Ziv & Tishby, 2017](#))¹⁴. In practice, due to floating point constraints such an optimization trajectory will invariably end in garbage predictions as activations approach zero and is therefore not desirable for training. This is why [Strouse & Schwab \(2017\)](#) only consider analytical solutions to DIB by evaluating a limit. Another more conceptual solution to this issue is adding noise ([MacKay, 2003](#)).

We also propose adding noise to the latent representation to lower-bound entropies and enforce non-negativity across all information quantities as in the discrete case: for a continuous \hat{Z} and independent noise ϵ , we set $Z := \hat{Z} + \epsilon$. The differential entropy satisfies $H[Z] = H[\hat{Z} + \epsilon] \geq H[\epsilon]$ and by using zero-entropy noise $\epsilon \sim \mathcal{N}(0, \frac{1}{2\pi e})$ specifi-

¹⁴Similarly, [MacKay \(2003\)](#) notes that without upper-bounding the “power” $\mathbb{E}_{p(z)} Z^2$, all information could be encoded in a single very large integer.

cally, we have $H[\epsilon] = 0$ and obtain

$$H[Z] \geq H[\epsilon] = 0.$$

Observation 6. *After adding zero-entropy noise, the inequality $I[X; Z | Y] \leq H[Z | Y] \leq H[Z]$ also holds in the continuous case, and we can minimize $I[X; Z | Y]$ in the IB objective by minimizing $H[Z | Y]$ or $H[Z]$, similarly to the DIB objective.*

We present a formal proof in section A.5 in the appendix.

By adding zero-entropy noise to Z , we ensure that all information quantities are non-negative and inequalities transfer to the continuous case. Furthermore, we bound the IB objective by the DIB objective. Adding noise changes the optimal solutions compared to Strouse & Schwab (2017): whereas DIB in Strouse & Schwab (2017) leads to hard clustering in the limit, adding noise leads to soft clustering when optimizing the DIB objective, as is the case with the IB objective. In section A.8 in the appendix, we show that minimizing equation DIB with noise also leads to soft clustering (at least for the case of an otherwise deterministic encoder). Altogether, in addition to Shwartz-Ziv & Tishby (2017), we argue that noise is essential to obtain meaningful differential entropies and to avoid pathological cases¹⁵.

6.2 Upper-Bounding $H[Z | Y]$

It is not generally possible to compute $H[Z | Y]$ exactly for continuous latent representations Z . However, the maximum-entropy distribution for a given covariance Σ is Gaussian with the same covariance, so we can derive an upper bound.

Observation 7. *The empirical variance $\widehat{\text{Var}}[Z_i | y]$ can be used to obtain an approximate upper bound on the Reverse Decoder Uncertainty:*

$$H[Z | Y] \lesssim \mathbb{E}_{\hat{p}(y)} \sum_i \frac{1}{2} \ln(2\pi e \widehat{\text{Var}}[Z_i | y]).$$

We derive this result as follows:

$$\begin{aligned} H[Z | Y] &= \mathbb{E}_{\hat{p}(y)} H[Z | y] \\ &\leq \mathbb{E}_{\hat{p}(y)} \frac{1}{2} \ln \det(2\pi e \text{Cov}[Z | y]) \\ &\leq \mathbb{E}_{\hat{p}(y)} \sum_i \frac{1}{2} \ln(2\pi e \text{Var}[Z_i | y]) \\ &\approx \mathbb{E}_{\hat{p}(y)} \sum_i \frac{1}{2} \ln(2\pi e \widehat{\text{Var}}[Z_i | y]), \end{aligned}$$

where Z_i are the individual components of Z and $\widehat{\text{Var}}[Z_i | y]$ is the sample variance. See section A.6 in the appendix for a more formal proof. We can bound $H[Z]$ similarly.

¹⁵See also section A.4 in the appendix.

The looseness of this bound will depend on how closely the mean-field Gaussian assumption matches the true distribution of the activations of the latent representation. While an appeal to the central limit theorem suggests that for a stochastic neural network, the distribution of a sampled mean activation will approach a Gaussian in the limit of samples, $P(Z|Y)$ is almost certainly multimodal. Thus, one expects the multi-modality of Z to be a significant factor in the tightness of a variance-based upper bound on entropy.

More generally, we can create an even looser upper-bound by bounding the mean squared norm of the latent:

$$\mathbb{E} \|Z\|^2 \leq C' \Rightarrow H[Z | Y] \leq H[Z] \leq C,$$

with $C' := \frac{e^{2C}}{2\pi e}$. We can thus replace the regularization term with $\mathbb{E} \|Z\|^2$ directly. This might seem like a very loose bound, but one can show that this is the entropy regularizer that Alemi et al. (2016) are using¹⁶. See section A.7 in the appendix for details.

This provides us with three different upper-bounds that we can use as surrogate regularizers. We refer to them as: conditional log-variance regularizer ($\log \text{Var}[Z | Y]$), log-variance regularizer ($\log \text{Var}[Z]$) and activation L_2 regularizer ($\mathbb{E} \|Z\|^2$).

6.3 Surrogate Objectives

Using the results above, we can now propose the main results of this paper: IB surrogate objectives that reduce to an almost trivial implementation using the cross-entropy loss and one of the regularizers above while adding zero-entropy noise to Z .

Observation 8. *As surrogate objective for $\mathbb{E} \|Z\|^2$, we have*

$$\min H_{\Theta}[Y | Z] + \gamma \mathbb{E} \|Z\|^2;$$

for $\log \text{Var}[Z | Y]$,

$$\min H_{\Theta}[Y | Z] + \gamma \mathbb{E}_{\hat{p}(y)} \sum_i \frac{1}{2} \ln(2\pi e \widehat{\text{Var}}[Z_i | y]);$$

and for $\log \text{Var}[Z]$, respectively,

$$\min H_{\Theta}[Y | Z] + \gamma \sum_i \frac{1}{2} \ln(2\pi e \widehat{\text{Var}}[Z_i]),$$

where we add zero-entropy noise to the latent, and where we estimate the Decoder Cross-Entropy $H_{\Theta}[Y | Z] = H(p(y | z) \| p_{\Theta}(\tilde{Y} = y | z))$ using the regular cross-entropy while using a single Dropout sample during training (or a deterministic model) as discussed in section 5.3.

¹⁶Alemi et al. (2016) model $H[Z | X]$ specifically and regularize with $\mathbb{E} \|Z\|^2 - H[Z | X]$.

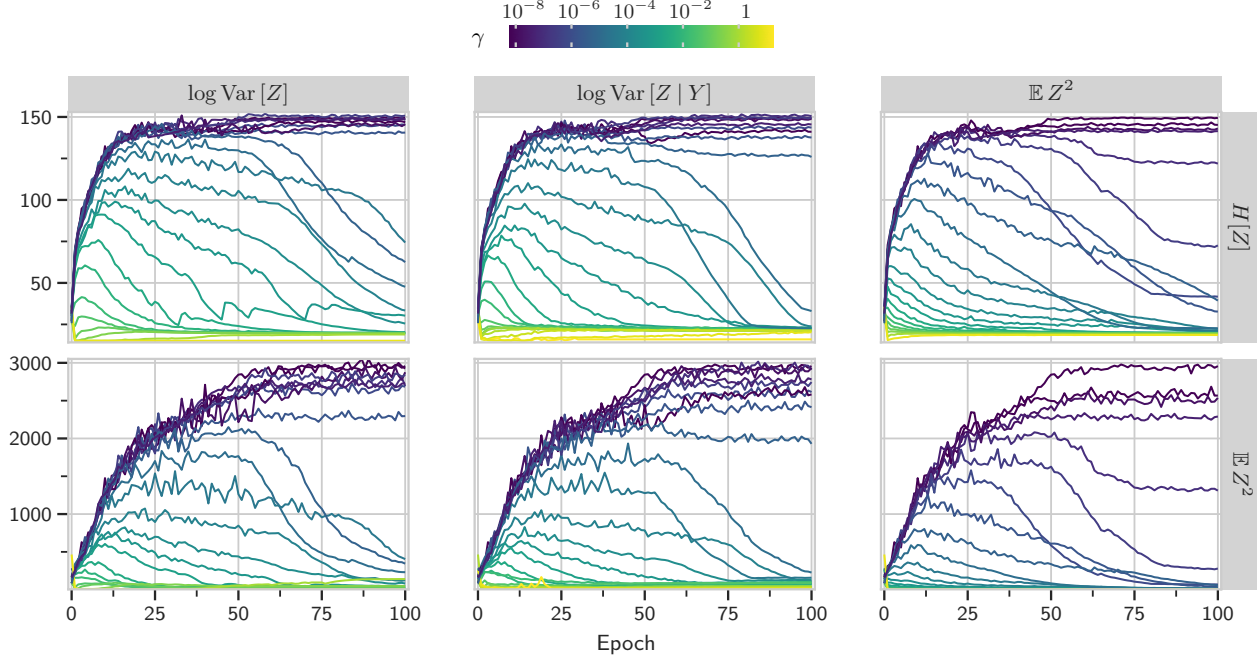


Figure 5: Entropy estimates while training with different γ and with different surrogate regularizers on CIFAR10 with a ResNet18 model. Entropies are estimated on training data based on Kraskov et al. (2004). Qualitatively all three regularizers push $H[Z]$ and $H[Z|Y]$ down. $H[Z|Y]$ is not shown here because it is always very close to $H[Z|X]$. $E||Z||^2$ tends to regularize entropies more strongly for small γ . See section 7.3 for more details.

We can relate the hyperparameter γ to β' , β'' and β from section 4.3. As regularizing $E||Z||^2$ does not approximate an entropy directly, its hyperparameter does not directly relate to any of the other hyperparameters. We compare the performance of these objectives in section 7.3.

7 Experiments

We now provide empirical verification of the claims made in the previous sections. We first describe experiments in section 7.1 that show that the Decoder Cross-Entropy upper-bounds the Decoder Uncertainty and Prediction Cross-Entropy as predicted in section 5. We use a categorical latent to be able to compute the optimal decoder $p(y|z)$ and Decoder Uncertainty $H[Y|Z]$ as described in section 5.4. We then give evidence in section 7.2 that minimizing $H[Z|Y]$ for continuous latent Z without adding noise does not constrain the information meaningfully and that adding noise solves the issue as discussed in section 6.1. Finally, we show in section 7.3 that adding noise and minimizing the surrogate objectives introduced in section 6 optimizes IB objectives. We show this by recovering Information Plane Plots similar to the ones in Tishby & Zaslavsky (2015) and investigate the trajectories during training to qualitatively examine the dynamics of the networks during training.

For our experiments, we use PyTorch (Paszke et al., 2019). We use the Adam optimizer with initial learning rate 10^{-4} (Kingma & Ba, 2014). We lower the learning rate by 0.8 whenever it plateaus for more than 3 epochs.

7.1 The Gap between Decoder Uncertainty and Decoder Cross-Entropy is small

To provide answers for the question posed in section 5 about the size of the gap between Decoder Uncertainty and Decoder Cross-Entropy and the training behavior of the two cross-entropies, we examine Permutation MNIST and CIFAR10 with categorical Z . For Permutation MNIST (Goodfellow et al., 2013), we use the common fully-connected ReLU 784 – 1024 – 1024 – C encoder architecture, with $C = 100$ categories for Z . For CIFAR10 (Krizhevsky et al., 2009), we use a standard ResNet18 model with C many output classes as encoder (He et al., 2016). Even though a $C \times 10$ matrix and a SoftMax would suffice to describe the decoder matrix $p_\theta(\hat{y}|z)$ ¹⁷, we have found that over-parameterization using a separate DNN benefits optimization a lot. Thus, to parameterize the decoder matrix, we use fully-connected ReLUs $C - 1024 - 1024 - 10$ with a final SoftMax layer.

¹⁷For categorical Z , $p_\theta(\hat{y}|z)$ is a stochastic matrix which sums to 1 along the \hat{Y} dimension.

We compute it once per batch during training and back-propagate into it.

Figure 3 shows the three metrics as we train with each of them in turn. Our results do not achieve SOTA accuracy on the test set—we impose a harder optimization problem as Z is categorical, and we are essentially solving a hard-clustering problem first and then map these clusters to \hat{Y} . We achieve about 98% accuracy on the test set. Results are provided for the training set in order to be able to compare with the optimal decoder.

As predicted, the **Decoder Cross-Entropy** upper-bounds both the **Decoder Uncertainty** $H[Y | Z]$ and the **Prediction Cross-Entropy** in all cases. Likewise, the gap between $H_\theta[Y | Z]$ and $H[Y | Z]$ is tiny when we minimize $H_\theta[Y | Z]$. On the other hand, minimizing **Prediction Cross-Entropy** can lead to large gaps between $H_\theta[Y | Z]$ and $H[Y | Z]$, as can be seen for CIFAR10.

Very interestingly, on MNIST **Decoder Cross-Entropy** provides a better training objective whereas on CIFAR10 **Prediction Cross-Entropy** trains lower. **Decoder Uncertainty** does not train very well on CIFAR10, and **Prediction Cross-Entropy** does not train well on Permutation MNIST at all. We suspect DNN architectures in the literature have evolved to train well with cross-entropies, but we are surprised by the heterogeneity of the results for the two datasets and models.

7.2 Differential Entropies Need Noise

Regularization only makes sense when it has an effect on the model. To show that one can arbitrarily minimize entropy without having an effect on the model when not adding noise, we use MNIST with a standard Dropout CNN (as provided by the PyTorch examples) as encoder (with $K = 128$ continuous dimensions instead of 10 in the last fully-connected layer) and a $K \times 10$ linear unit as decoder with 12 Dropout samples. After every training epoch, we decrease the entropy of the latent by normalizing it and then scaling it to bound the entropy. We multiply the weights of the decoder to not impact performance unnecessarily. As can be seen in figure 4, without noise, entropy can decrease freely during training without change in error rate until it is affected by floating-point issues; while when adding zero-entropy noise, the error rate starts increasing gradually and meaningfully as the entropy starts to approach zero.

7.3 Surrogate Regularizers Work

To compare the different surrogate regularizers, we use a standard ResNet18 model on CIFAR10 with zero-entropy noise added to the final layer activations Z with $K = 100$ dimensions as encoder and add a single $K \times 10$ linear

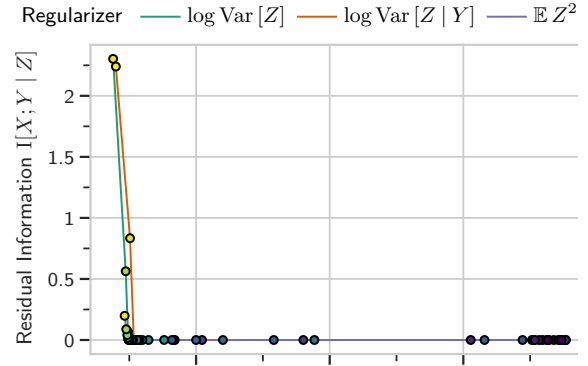


Figure 6: *Information Plane Plot of the latent Z similar to Tishby & Zaslavsky (2015) but using a ResNet18 model on CIFAR10 using the different regularizes from section 6.3. The dots are colored by γ . See section 7.3 for more details.*

unit as decoder. We use the different surrogate objectives from section 6.3. γ varies from 10^{-4} to 10 in log space. We use estimators based on Kraskov et al. (2004) for the information quantities. One Dropout sample has been found to be sufficient as it is an unbiased estimator of the **Decoder Cross-Entropy**. We drop the learning rate whenever it plateaus for more than 10 epochs.

As can be seen in figure 5, the different surrogate regularizers have very similar effects on $H[Z]$ and $H[Z | Y]$. Regularizing with $\mathbb{E} \|Z\|^2$, shows a stronger initial regularization effect and is difficult to compare quantitatively as its hyperparameter does not map to β unlike regularizing using entropy estimates, which allows us to map γ to the hyperparameters β' and β'' from section 4.3. In figure 6, we can see that the saturation curves for all 3 surrogate objectives qualitatively match the predicted curve from Tishby & Zaslavsky (2015)¹⁸.

Finally, figure 1 shows an Information Plane plot for the model for different γ over different epochs for the training set. Similar to Shwartz-Ziv & Tishby (2017), we observe that there is an initial expansion phase followed by compression. The jumps in performance (reduction of **Residual Information**) are due to drops in the learning rate¹⁹.

¹⁸Figure 7 in the appendix shows the difference between the regularizers more clearly.

¹⁹Figure 8 in the appendix shows the training trajectories for all three regularizers.

8 Conclusion

The contributions of this paper have been threefold: First, we have provided mathematically grounded intuition by using I-diagrams for the information quantities involved in IB, shown common pitfalls when using information quantities and how to avoid them, and examined how the quantities relate to each other.

Second, we have endeavoured to provide a unifying view on IB approaches and further provided insight into limitations of IB training, demonstrating how to avoid pathological behavior in IB objectives.

Third, we have demonstrated that relatively simple training objectives based on this intuition can capture many of the desirable properties of IB methods while also scaling to problems of interest in deep learning. Specifically, we have shown how the [Decoder Uncertainty](#) relates to the cross-entropy loss that is commonly used for classification problems, and that we can move beyond toy examples using IB methods to more practical DNNs without heavy lifting and generative models. Future work investigating how the practical constraints on the expressivity of a given neural network may provide further insight into how to measure compression in neural networks, and potentially yield improved regularizers over those presented in this paper.

Acknowledgements

The authors want to thank Lewis Smith, Joost van Amersfoort, Maximilian Igl and Tim Rudner for helpful discussions and feedback. We would also like to thank the rest of OATML for their feedback at several stages of the project. AK is supported by the UK EPSRC CDT in Autonomous Intelligent Machines and Systems (grant reference EP/L015897/1).

References

- Achille, A. and Soatto, S. Emergence of invariance and disentanglement in deep representations. *The Journal of Machine Learning Research*, 19(1):1947–1980, 2018a.
- Achille, A. and Soatto, S. Information dropout: Learning optimal representations through noisy computation. *IEEE transactions on pattern analysis and machine intelligence*, 40(12):2897–2905, 2018b.
- Alemi, A. A., Fischer, I., Dillon, J. V., and Murphy, K. Deep variational information bottleneck. *arXiv preprint arXiv:1612.00410*, 2016.
- Amjad, R. A. and Geiger, B. C. Learning representations for neural network-based classification using the information bottleneck principle. *IEEE Transactions on Pattern Analysis and Machine Intelligence*, 2019.
- Belghazi, M. I., Baratin, A., Rajeshwar, S., Ozair, S., Bengio, Y., Courville, A., and Hjelm, D. Mutual information neural estimation. In *International Conference on Machine Learning*, pp. 531–540, 2018.
- Bercher, J.-F. and Vignat, C. A renyi entropy convolution inequality with application. In *2002 11th European Signal Processing Conference*, pp. 1–4. IEEE, 2002.
- Burda, Y., Grosse, R., and Salakhutdinov, R. Importance weighted autoencoders. *arXiv preprint arXiv:1509.00519*, 2015.
- Cover, T. M. and Thomas, J. A. *Elements of information theory*. John Wiley & Sons, 2012.
- Fisher, I. The Conditional Entropy Bottleneck. *Submission to ICLR 2019, International Conference on Learning Representations*, 2019.
- Gal, Y. and Ghahramani, Z. Dropout as a bayesian approximation: Representing model uncertainty in deep learning. In *international conference on machine learning*, pp. 1050–1059, 2016.
- Gondek, D. and Hofmann, T. Conditional information bottleneck clustering. In *3rd ieee international conference on data mining, workshop on clustering large data sets*, pp. 36–42. Citeseer, 2003.
- Goodfellow, I. J., Mirza, M., Xiao, D., Courville, A., and Bengio, Y. An empirical investigation of catastrophic forgetting in gradient-based neural networks. *arXiv preprint arXiv:1312.6211*, 2013.
- He, K., Zhang, X., Ren, S., and Sun, J. Deep residual learning for image recognition. In *Proceedings of the IEEE conference on computer vision and pattern recognition*, pp. 770–778, 2016.
- Houlsby, N., Huszár, F., Ghahramani, Z., and Lengyel, M. Bayesian active learning for classification and preference learning. *arXiv preprint arXiv:1112.5745*, 2011.
- Inoue, H. Multi-sample dropout for accelerated training and better generalization. *arXiv preprint arXiv:1905.09788*, 2019.
- Kingma, D. P. and Ba, J. Adam: A method for stochastic optimization. *arXiv preprint arXiv:1412.6980*, 2014.
- Kirsch, A., van Amersfoort, J., and Gal, Y. Batchbald: Efficient and diverse batch acquisition for deep bayesian active learning. In *Advances in Neural Information Processing Systems*, pp. 7024–7035, 2019.
- Kraskov, A., Stögbauer, H., and Grassberger, P. Estimating mutual information. *Physical review E*, 69(6): 066138, 2004.
- Krizhevsky, A., Hinton, G., et al. Learning multiple layers of features from tiny images. 2009.

- MacKay, D. J. C. *Information Theory, Inference, and Learning Algorithms*. Cambridge University Press, 2003.
- McAllester, D. and Stratos, K. Formal limitations on the measurement of mutual information. *arXiv preprint arXiv:1811.04251*, 2018.
- McGill, W. Multivariate information transmission. *Transactions of the IRE Professional Group on Information Theory*, 4(4):93–111, 1954.
- Noh, H., You, T., Mun, J., and Han, B. Regularizing deep neural networks by noise: Its interpretation and optimization. In *Advances in Neural Information Processing Systems*, pp. 5109–5118, 2017.
- Noshad, M., Zeng, Y., and Hero, A. O. Scalable mutual information estimation using dependence graphs. In *ICASSP 2019-2019 IEEE International Conference on Acoustics, Speech and Signal Processing (ICASSP)*, pp. 2962–2966. IEEE, 2019.
- Oord, A. v. d., Li, Y., and Vinyals, O. Representation learning with contrastive predictive coding. *arXiv preprint arXiv:1807.03748*, 2018.
- Paszke, A., Gross, S., Massa, F., Lerer, A., Bradbury, J., Chanan, G., Killeen, T., Lin, Z., Gimelshein, N., Antiga, L., et al. Pytorch: An imperative style, high-performance deep learning library. In *Advances in Neural Information Processing Systems*, pp. 8024–8035, 2019.
- Poole, B., Ozair, S., Oord, A. v. d., Alemi, A. A., and Tucker, G. On variational bounds of mutual information. *arXiv preprint arXiv:1905.06922*, 2019.
- Saxe, A. M., Bansal, Y., Dapello, J., Advani, M., Kolchinsky, A., Tracey, B. D., and Cox, D. D. On the information bottleneck theory of deep learning. *Journal of Statistical Mechanics: Theory and Experiment*, 2019 (12):124020, 2019.
- Shamir, O., Sabato, S., and Tishby, N. Learning and generalization with the information bottleneck. *Theoretical Computer Science*, 411(29-30):2696–2711, 2010.
- Shannon, C. E. A mathematical theory of communication. *Bell system technical journal*, 27(3):379–423, 1948.
- Shwartz-Ziv, R. and Tishby, N. Opening the black box of deep neural networks via information. *arXiv preprint arXiv:1703.00810*, 2017.
- Srivastava, N., Hinton, G., Krizhevsky, A., Sutskever, I., and Salakhutdinov, R. Dropout: a simple way to prevent neural networks from overfitting. *The journal of machine learning research*, 15(1):1929–1958, 2014.
- Strouse, D. and Schwab, D. J. The deterministic information bottleneck. *Neural computation*, 29(6):1611–1630, 2017.
- Tishby, N. and Zaslavsky, N. Deep learning and the information bottleneck principle. In *2015 IEEE Information Theory Workshop (ITW)*, pp. 1–5. IEEE, 2015.
- Tishby, N., Pereira, F. C., and Bialek, W. The information bottleneck method. *arXiv preprint physics/0004057*, 2000.
- Tschannen, M., Djolonga, J., Rubenstein, P. K., Gelly, S., and Lucic, M. On mutual information maximization for representation learning. *arXiv preprint arXiv:1907.13625*, 2019.
- Yeung, R. W. A new outlook on shannon’s information measures. *IEEE transactions on information theory*, 37(3):466–474, 1991.
- Zhang, Y., Xiang, T., Hospedales, T. M., and Lu, H. Deep mutual learning. In *Proceedings of the IEEE Conference on Computer Vision and Pattern Recognition*, pp. 4320–4328, 2018.

A Appendix

A.1 Definitions & Equivalences

Definitions from section 3.2:

$$I[X; Y] = I[X; Y | Z] + I[Y; Z] \quad (6)$$

$$I[X; Z] = I[X; Z | Y] + I[Y; Z] \quad (7)$$

$$H[Y | Z] = I[X; Y | Z] + H[Y | X] \quad (8)$$

$$H[Z | Y] = I[X; Z | Y] + H[Z | X] \quad (9)$$

$$H[X | Y] = H[X | Y, Z] + I[X; Z] \quad (10)$$

We can combine the atomic quantities into our overall **Label Entropy** and **Encoding Entropy**:

$$H[Y] = H[Y | X] + I[Y; Z] + I[X; Y | Z] \quad (11)$$

$$H[Z] = H[Z | X] + I[Y; Z] + I[X; Z | Y]. \quad (12)$$

We can express the **Relevant Information** $I[X; Y]$, **Residual Information** $I[X; Y | Z]$, **Redundant Information** $I[X; Z | Y]$ and **Preserved Information** $I[X; Z]$ without X on the left-hand side:

$$I[X; Y] = H[Y] - H[Y | X], \quad (13)$$

$$I[X; Z] = H[Z] - H[Z | X], \quad (14)$$

$$I[X; Y | Z] = H[Y | Z] - H[Y | X], \quad (15)$$

$$I[X; Z | Y] = H[Z | Y] - H[Z | X]. \quad (16)$$

This simplifies estimating these expressions as X is usually much higher-dimensional and irregular than our labels or latent encodings. We also can rewrite the **Preserved Relevant Information** $I[Y; Z]$ as:

$$I[Y; Z] = H[Y] - H[Y | Z] \quad (17)$$

$$I[Y; Z] = H[Z] - H[Z | Y] \quad (18)$$

A.2 IB and the Entropy Distance Metric

Another perspective on the IB objectives is by expressing them using the Entropy Distance Metric. MacKay (2003, p. 140) introduces the entropy distance

$$EDM(Y, Z) = H[Y | Z] + H[Z | Y]. \quad (19)$$

as a metric when we identify random variables up to permutations of the labels for categorical variables: if the entropy distance is 0, Y and Z are the same distribution up to a consistent permutation of the labels (independent of X). If the entropy distance becomes 0, both $H[Y | Z] = 0 = H[Z | Y]$, and we can find a bijective map from Z to Y .²⁰

²⁰The argument for continuous variables is the same. We need to identify distributions up to “isentropic” bijections.

We can express the **Reverse Decoder Uncertainty** $H[Z | Y]$ using the **Decoder Uncertainty** $H[Y | Z]$ and the entropies:

$$H[Z | Y] + H[Y] = H[Y | Z] + H[Z], \quad (20)$$

and rewrite equation 19 as

$$EDM(Y, Z) = 2H[Y | Z] + H[Z] - H[Y]. \quad (21)$$

For optimization purposes, we can drop constant terms and rearrange:

$$\arg \min EDM(Y, Z) = \arg \min H[Y | Z] + \frac{1}{2}H[Z]. \quad (22)$$

A.2.1 Rewriting IB and DIB using the Entropy Distance Metric

For $\beta \geq 1$, we can rewrite equation IB and equation DIB as:

$$\begin{aligned} \arg \min EDM(Y, Z) + \gamma(H[Y | Z] - H[Z | Y]) \\ + (\gamma - 1)H[Z | X] \end{aligned} \quad (23)$$

for IB, and

$$\arg \min EDM(Y, Z) + \gamma(H[Y | Z] - H[Z | Y]) \quad (24)$$

for DIB and replace β with $\gamma = 1 - \frac{2}{\beta} \in [-1, 1]$ which allows for a linear mix between $H[Y | Z]$ and $H[Z | Y]$.

DIB will encourage the model to match both distributions for $\gamma = 0$ ($\beta = 2$), as we obtain a term that matches the Entropy Distance Metric from section A.2, and otherwise trades off **Decoder Uncertainty** and **Reverse Decoder Uncertainty**. IB behaves similarly but tends to maximize **Encoding Uncertainty** as $\gamma - 1 \in [-2, 0]$. Fisher (2019) argues for picking this configuration similar to the arguments in section 4.1. DIB will force both distributions to become exactly the same, which would turn the decoder into a permutation matrix for categorical variables.

A.3 Gradient of the Decoder Uncertainty $H[Y | Z]$

We have:

$$\frac{d}{d\theta} H[Y | Z] = \mathbb{E}_{p(x,z)} \left[\frac{d}{d\theta} [\ln p_{\Theta}(z | x)] \mathbb{E}_{p(y|x)} h(p(y | z)) \right].$$

Proof.

$$\begin{aligned} \frac{d}{d\theta} H[Y | Z] &= \frac{d}{d\theta} \mathbb{E}_{p(y,z)} h(p(y | z)) \\ &= \frac{d}{d\theta} \mathbb{E}_{p(x,y,z)} h(p(y | z)) \\ &= \mathbb{E}_{p(x,y)} \frac{d}{d\theta} \mathbb{E}_{p_{\Theta}(z|x)} h(p(y | z)) \end{aligned}$$

$$\begin{aligned}
&= \mathbb{E}_{p_{\Theta}(z|x)} \mathbb{E}_{\hat{p}(x,y)} \frac{d}{d\theta} [h(p(y|z))] + \\
&\quad h(p(y|z)) \frac{d}{d\theta} [\ln p_{\Theta}(z|x)] \\
&= \mathbb{E}_{p(x,y,z)} \frac{d}{d\theta} [h(p(y|z))] + \\
&\quad h(p(y|z)) \frac{d}{d\theta} [\ln p_{\Theta}(z|x)].
\end{aligned}$$

And now we show that $\mathbb{E}_{p(x,y,z)} \frac{d}{d\theta} [h(p(y|z))] = 0$:

$$\begin{aligned}
\mathbb{E}_{p(x,y,z)} \frac{d}{d\theta} [h(p(y|z))] &= \\
&= \mathbb{E}_{p(y,z)} \frac{d}{d\theta} [h(p(y|z))] \\
&= \mathbb{E}_{p(y,z)} \frac{-1}{p(y|z)} \frac{d}{d\theta} p(y|z) \\
&= - \int \frac{p(y,z)}{p(y|z)} \frac{d}{d\theta} p(y|z) dy dz \\
&= - \int p(z) \int \frac{d}{d\theta} p(y|z) dy dz \\
&= - \int p(z) \frac{d}{d\theta} \underbrace{\left[\int p(y|z) dy \right]}_{=1} dz = 0.
\end{aligned}$$

Splitting the expectation and reordering of $\mathbb{E}_{p(x,y,z)} h(p(y|z)) \frac{d}{d\theta} [\ln p_{\Theta}(z|x)]$, we obtain the result. \square

This is the same as maximizing a weighted cross-entropy of $p_{\Theta}(z|x)$ with weights $\mathbb{E}_{p(y|x)} h(p(y|z))$, which is pushing the probability of unlikely latent encodings $p_{\Theta}(z|x)$ towards 0.

The same holds for **Reverse Decoder Uncertainty** $H[Z|Y]$ and for the other quantities as can be verified.

A.4 A Note on Differential and Discrete Entropies

The mutual information between two random variables can be defined in terms of the KL divergence between the product of their marginals and their joint distribution. However, the KL divergence is only well-defined when the Radon-Nikodym derivative of the density of the joint with respect to the product exists. Mixing continuous and discrete distributions—and thus differential and continuous entropies—can violate this requirement, and so lead to negative values of the “mutual information”. This is particularly worrying in the setting of training stochastic neural networks, as we often assume that a stochastic embedding is generated as a deterministic transformation of an input from a finite dataset to which a continuous perturbation is added. We provide an examples where naive computation without ensuring that the product and joint distributions of the two random variables have a

well-defined Radon-Nikodym derivative yields negative mutual information.

Let $X \sim U([0, 0.1])$, $Z = X + R$ with $R \sim U(\{0, 1\})$. Then

$$I[X; Z] = H[X] = \log \frac{1}{10} \leq 0.$$

Similarly, given X as above and an invertible function f such that $Z = f(X)$, $I[X; Z]$ is not defined.

We can avoid these cases by adding independent continuous noise.

These two examples show that not adding noise can lead to unexpected results. While they still yield finite quantities that bear a relation to the entropies of the random variables, they violate some of the core assumptions we have such that mutual information is always positive.

A.5 Differential Entropies

Theorem 1. For random variables A, B , we have

$$H[A + B] \geq H[B].$$

Proof. See Bercher & Vignat (2002, section 2.2). \square

Proposition 1. Let Y, Z and X be random variables satisfying the independence property $Z \perp Y|X$, and F a possibly stochastic function such that $Z = F(X) + \epsilon$, with independent noise ϵ satisfying $\epsilon \perp F(X), \epsilon \perp Y$ and $H(\epsilon) = 0$. Then the following holds whenever $I[Y; Z]$ is well-defined.

$$I[X; Z|Y] \leq H[Z|Y] \leq H[Z].$$

Proof. First, we note that $H[Z|X] = H[F(X) + \epsilon|X] \geq H[\epsilon|X] = H[\epsilon]$ with theorem 1, as ϵ is independent of X , and thus $H[Z|X] \geq 0$. We have $H[Z|X] = H[Z|X, Y]$ by the conditional independence assumption, and by the non-negativity of mutual information, $I[Y; Z] \geq 0$. Then:

$$\begin{aligned}
I[X; Z|Y] + \underbrace{H[Z|X]}_{\geq 0} &= H[Z|Y] \\
H[Z|Y] + \underbrace{I[Y; Z]}_{\geq 0} &= H[Z]
\end{aligned}$$

\square

The probabilistic model from section 3 fulfills the conditions exactly.

A.6 Upper-Bounding $H[Z|Y]$

Theorem 2. Given a k -dimensional random variable $X = (X_i)_{i=1}^k$ with $\text{Var}[X_i] > 0$ for all i ,

$$H[X] \leq \frac{1}{2} \ln \det(2\pi e \text{Cov}[X])$$

$$\leq \sum_i \frac{1}{2} \ln(2\pi e \text{Var}[X_i]).$$

Proof. First, the multivariate normal distribution with same covariance is the maximum entropy distribution for that covariance, and thus $H[X] \leq \ln \det(2\pi e \text{Cov}[X])$, when we substitute the differential entropy for a multivariate normal distribution with covariance $\text{Cov}[X]$. Let $\Sigma_0 := \text{Cov}[X]$ be the covariance matrix and $\Sigma_1 := \text{diag}(\text{Var}[X_i])_i$ the matrix that only contains the diagonal. Because we add independent noise, $\text{Var}[X_i] > 0$ and thus Σ_1^{-1} exists. It is clear that $\text{tr}(\Sigma_1^{-1}\Sigma_0) = k$. Then, we can use the KL-Divergence between two multivariate normal distributions $\mathcal{N}_0, \mathcal{N}_1$ with same mean 0 and covariances Σ_0 and Σ_1 to show that $\ln \det \Sigma_0 \leq \ln \det \Sigma_1$:

$$\begin{aligned} 0 &\leq D_{\text{KL}}(\mathcal{N}_0 \parallel \mathcal{N}_1) = \frac{1}{2} \left(\text{tr}(\Sigma_1^{-1}\Sigma_0) - k + \ln \left(\frac{\det \Sigma_1}{\det \Sigma_0} \right) \right) \\ \Leftrightarrow 0 &\leq \frac{1}{2} \ln \left(\frac{\det \Sigma_1}{\det \Sigma_0} \right) \Leftrightarrow \frac{1}{2} \ln \det \Sigma_0 \leq \frac{1}{2} \ln \det \Sigma_1. \end{aligned}$$

We substitute the definitions of Σ_0 and Σ_1 , and obtain the second inequality after adding $k \ln(2\pi e)$ on both sides. \square

A.7 Alemi et al. (2016) and $\mathbb{E} \|Z\|^2$

Alemi et al. (2016) model $p(z|x)$ explicitly as output of their encoder and regularize it to become close to $\mathcal{N}(0, I_k)$ by minimizing the term $D_{\text{KL}}(p(z|x) \parallel \mathcal{N}(0, I_k))$ alongside the cross-entropy.

Overall the regularizer term becomes

$$\begin{aligned} D_{\text{KL}}(p(z|x) \parallel \mathcal{N}(0, I_k)) &= \mathbb{E}_{\hat{p}(x)} \mathbb{E}_{p(z|x)} h \left((2\pi)^{-\frac{k}{2}} e^{-\frac{1}{2}\|Z\|^2} \right) - H[Z|X] \\ &= \mathbb{E}_{p(z)} \left[\frac{k}{2} \ln(2\pi) + \frac{1}{2}\|Z\|^2 \right] - H[Z|X]. \end{aligned}$$

We can drop the constant term and obtain

$$= \frac{1}{2} \mathbb{E} \|Z\|^2 - H[Z|X].$$

A.8 Soft Clustering by Entropy Minimization with Gaussian Noise

Consider the problem of minimizing $H[Z|Y]$ and $H[Y|Z]$, in the setting where $Z = f_\Theta(X) + \epsilon \sim \mathcal{N}(0, \sigma^2)$ —i.e. the embedding Z is obtained by adding Gaussian noise to a deterministic function of the input. Let the training set be enumerated x_1, \dots, x_n , with $\mu_i = f_\Theta(x_i)$. Then the distribution of Z is given by a mixture of Gaussians with the following density, where $d(x, \mu_i) := \|x - \mu_i\|/\sigma^2$.

$$p(z) \propto \frac{1}{n} \sum_{i=1}^n \exp(-d(z, \mu_i))$$

Assuming that each x_i has a deterministic label y_i , we then find that the conditional distributions $p(y|z)$ and $p(z|y)$ are given as follows:

$$\begin{aligned} p(z|y) &\propto \frac{1}{n_y} \sum_{i:y_i=y} \exp(-d(z, \mu_i)) \\ p(y|z) &= \sum_{i:y_i=y} p(\mu_i|z) = \sum_{i:y_i=y} \frac{p(z|\mu_i) p(\mu_i)}{p(z)} \\ &= \frac{\sum_{i:y_i=y} p(z|\mu_i)}{\sum_{k=1}^n p(z|\mu_k)} = \frac{\sum_{i:y_i=y} \exp(-d(z, \mu_i))}{\sum_{k=1}^n \exp(-d(z, \mu_k))}, \end{aligned}$$

where n_y is the number of x_i with class $y_i = y$. Thus, the conditional $Z|Y$ can be interpreted as a mixture of Gaussians and $Y|Z$ as a Softmax marginal with respect to the distances between Z and the mean embeddings. We observe that $H[Z|Y]$ is lower-bounded by the entropy of the random noise added to the embeddings:

$$H[Z|Y] \geq H[f_\Theta(X) + \epsilon | Y] \geq H[\epsilon]$$

with equality when the distribution of $f_\Theta(X)|Y$ is deterministic—that is f_Θ is constant for each equivalence class.

Further, the entropy $H[Y|Z]$ is minimized when $H[Z]$ is large compared to $H[Z|Y]$ as we have the decomposition

$$H[Y|Z] = H[Z|Y] - H[Z] + H[Y].$$

In particular, when f_Θ is constant over equivalence classes of the input, then $H[Y|Z]$ is minimized when the entropy $H[f_\Theta(X) + \epsilon]$ is large—i.e. the values of $f_\Theta(x_i)$ for each equivalence class are distant from each other and there is minimal overlap between the clusters. Therefore, the optima of the information bottleneck objective under Gaussian noise share similar properties to the optima of geometric clustering of the inputs according to their output class.

To gain a better understanding of local optimization behavior, we decompose the objective terms as follows:

$$\begin{aligned} H[Z|Y] &= \mathbb{E}_{\hat{p}(y)} H(p(z|y) \parallel p(z|y)) \\ &= \mathbb{E}_{\hat{p}(x,y)} H(p(z|x) \parallel p(z|y)) \\ &= \mathbb{E}_{\hat{p}(x,y)} D_{\text{KL}}(p(z|x) \parallel p(z|y)) + H[Z|x] \\ &= \mathbb{E}_{\hat{p}(x,y)} D_{\text{KL}}(p(z|x) \parallel p(z|y)) \\ &\quad + \underbrace{H[Z|X]}_{=const}. \end{aligned}$$

To examine how the mean embedding μ_k of a single datapoint x_k affects this entropy term, we look at the derivative of this expression with respect to $\mu_k = f_\Theta(x_k)$. We obtain:

$$\frac{d}{d\mu_k} H[Z|Y] = \frac{d}{d\mu_k} H[Z|y_k]$$

$$\begin{aligned}
&= \frac{d}{d\mu_k} \mathbb{E}_{p(x|y_k)} D_{\text{KL}}(p(z|x) \| p(z|y)) \\
&= \sum_{i \neq k: y_i = y_k} \frac{1}{n_{y_k}} \frac{d}{d\mu_k} D_{\text{KL}}(p(z|x_i) \| p(z|y_k)) \\
&\quad + \frac{1}{n_{y_k}} \frac{d}{d\mu_k} D_{\text{KL}}(p(z|x_k) \| p(z|y_k)).
\end{aligned}$$

While these derivatives do not have a simple analytic form, we can use known properties of the KL divergence to develop an intuition on how the gradient will behave. We observe that in the left-hand sum μ_k only affects the distribution of $Z|Y$ (that is we are differentiating a sum of terms that look like a reverse KL), whereas it has greater influence on $p(z|x_k)$ in the right-hand term, and so its gradient will more closely resemble that of the forward KL. The left-hand-side term will therefore push μ_k towards the centroid of the means of inputs mapping to y , whereas the right-hand side term is mode-seeking.

A.9 Additional Plots

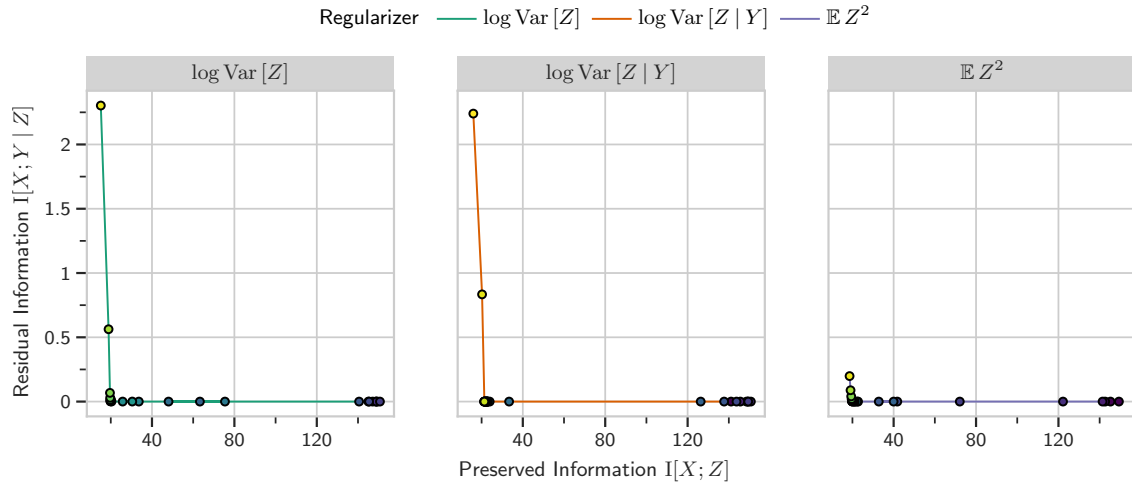


Figure 7: *Information Plane Plot of the latent Z similar to Tishby & Zaslavsky (2015) but using a ResNet18 model on CIFAR10 using the different regularizers from section 6.3. The dots are colored by γ . See section 7.3 for more details.*

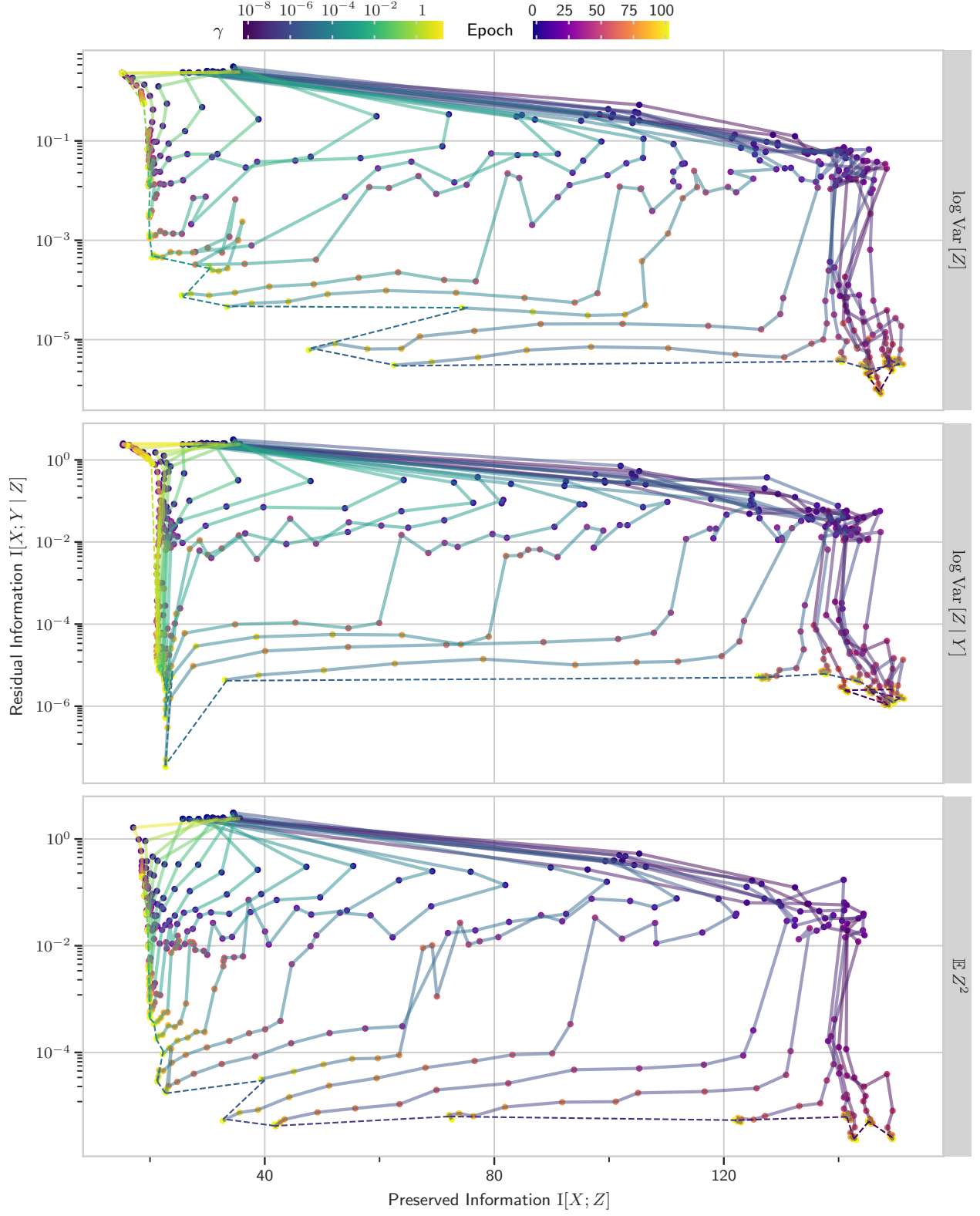


Figure 8: *Information Plane Plot of training trajectories for ResNet18 models on CIFAR10.* We use the surrogate objectives from section 6. Trajectories (for every 5th epoch) are plotted for different γ . The lines are colored by γ , the dots by epoch. The dashed line is the saturation curve depicted in figure 6. Depending on γ , different levels of compression (**Preserved Information** \downarrow) are achieved, which trade-off with performance (**Residual Information** \downarrow). See section 7.3.

A.10 Mickey Mouse I-Diagram

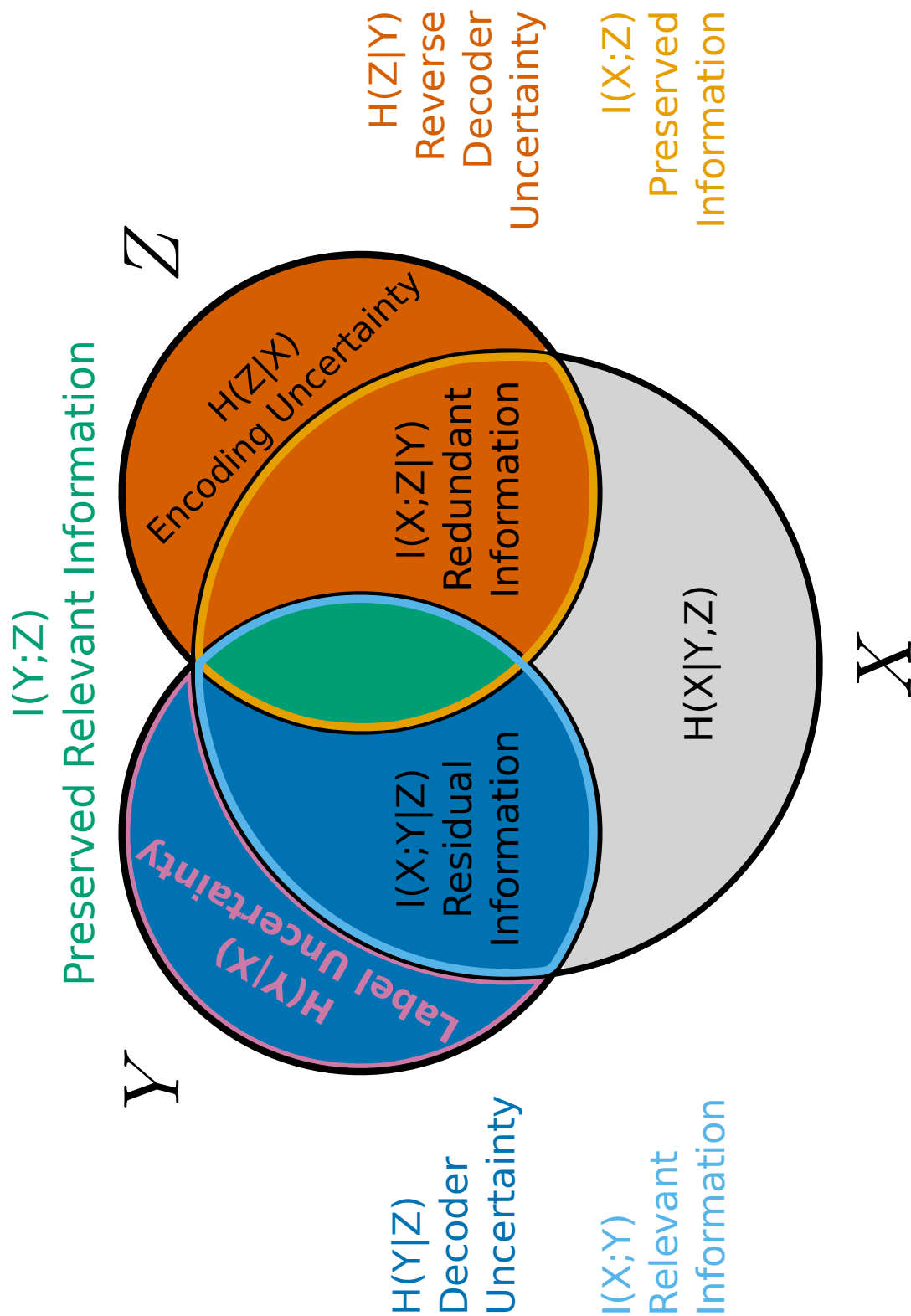


Figure 9: *Mickey Mouse I-diagram*. See figure 2 for details.